Eur. Phys. J. B (2014) 87: 61
DOI: 10.1140/epjb/e2014-40712-6

THE EUROPEAN PHYSICAL JOURNAL B

Regular Article

Ornstein-Zernike correlations and magnetic ordering in nanostructures

Ever Alberto Velásquez[1,2], Johan Mazo-Zuluaga[1,a], Dora Altbir[3], and José Mejía-López[4]

[1] GES and GICM Groups, Instituto de Física-FCEN, Universidad de Antioquia UdeA, Calle 70 No. 52-21, Medellín, Colombia
[2] Grupo de Investigación en Modelamiento y Simulación Computacional, Facultad de Ingenierías, Universidad de San Buenaventura Sec. Medellín, A.A. 5222 Medellín, Colombia
[3] Departamento de Física, Universidad de Santiago de Chile (USACH); CEDENNA, Santiago, Chile
[4] Facultad de Física, Pontificia Universidad Católica de Chile; CEDENNA, Santiago, Chile

Received 26 July 2013 / Received in final form 5 February 2014
Published online 10 March 2014 –

Abstract. In this paper we propose a Heisenberg variational approach to study pseudo-critical phenomena on ferromagnetic nanostructures. We combine a two-spin cluster 3-dimensional Heisenberg Hamiltonian with Orstein-Zernike correlations and consider several geometries and crystalline lattices to explore the relationship among these factors and the effective number of nearest neighbors defined in several kind of nanometric structures. With this method we examine the size at which the pseudo-critical temperature of a magnetic nanoparticle reaches its bulk value. Our results shed light on the nanoscopic-microscopic limit, evidencing in particular that when one dimension is very small, independently of how big the other dimensions become, it is not possible for the structure to reach the bulk-like behavior. The results of our model are in good agreement with experimental data and other available analytical models.

1 Introduction

During the last decades strong attention has been focused on nanostructures, mainly due to the great progress in experimental techniques that allow access to the nanometer length scales. Besides the basic scientific interest in particles at the nanoscale, there is evidence that they might be used in the production of interesting devices that can be useful in areas as diverse as health [1], electronic [2], food [3], and environment [4], among others. As the dimensions of a particle gradually decrease, the influence of dimensionality becomes a very important issue, and new properties appear which differ in many respects from what is observed in bulk structures. In particular, and regarding magnetic materials, the spontaneous magnetization, the magnetic order, the Curie and Néel temperatures and other properties exhibit important size effects which in some cases depend not only on the system's size but also on its shape.

An interesting work regarding size and shape effects was published by Skomski [5]. In that paper the author reviewed magnetic nanostructures such as dots, nanowires, multilayers and nanojunctions concluding that these structures exhibit important deviations from bulk magnets. One of the first geometries studied under this frame were thin films. For example, Lee et al. reported the critical temperature and the saturation magnetization of ultra thin iron films [6]. Later on Huang et al. [7] and Ambrose and Chien [8] reported finite size scaling in thin ferromagnetic and antiferromagnetic layers, respectively. More recently the magnetic properties of amorphous $Co_{40}Fe_{40}B_{20}$ thin films have been reported showing the impact of the size on the saturation magnetization and remanence [9].

Concerning nanoparticles, evidence of size-dependent behavior has been found in the study of antiferromagnetic Cr_2O_3 nanoparticles [10], where the Néel temperature and the spin-flip field increase with the particle size. These effects are the result of a surface disorder and spin canting that increase for smaller particles. Moshopoulou et al. investigated the size dependent behavior of the magnetization in $ZnFe_2O_4$ and conclude that nanoparticles of sizes larger than 100 nm exhibit a bulk like behavior [11]. Batlle et al. observed $Fe_{3-x}O_4$ nanoparticles whose bulk-like behavior is strongly linked to the crystal quality of the samples [12]. Also, evidence of size-dependent behavior has been found in the study of $Co_xFe_{2-x}O_3$ ($x = 0$, 0.06) nanoparticles with diameters between 20 and 100 nm [13]. In these particles the saturation magnetization was measured and an empirical linear dependence on the specific surface area of the crystallites was found.

Besides thin films and nanoparticles, there are several studies regarding size effects in nanowires. In particular Sun et al. studied nickel nanowire arrays with diameters in the range 30–500 nm and observe a strong reduction of the Curie temperature for the thinner wires that obeys a scaling relation [14,15]. Similar arrays were produced and

[a] e-mail: johanmazo@gmail.com

characterized by Meir et al. showing a strong dependence of the coercivity on the diameter of the wires and on the temperature [16].

From another side, interesting work has focused on the search for a universal definition of the characteristics that systems may have in order to exhibit properties associated with a nanometric behavior. In particular, we can mention a paper by Krishna et al. [17], where the authors showed that the chemical potential of bosons trapped in a harmonic potential shows a discontinuity as a function of the number of particles in the system. The same authors claimed that the transition from bulk-to-nanophase of a material is a first order phase transition [18]. Thus, finding the precise size at which particles evidence properties on the nanoscale becomes an interesting challenge.

The idea of relating magnetization and temperature for small particles has been previously explored by other authors under the frame of the Ising model. In particular, Bertoldi et al. used an Ising model for finite systems under the mean field approximation and found that the critical temperature follows a finite scaling that indicates that it decreases proportionally to the inverse of the radius of the particle [19]. Also Velásquez et al. [20] used the same model with a free-energy variational principle based on the Bogoliubov inequality [21–23] and obtained a size dependence for the ordering temperature that compared with experiments. However they obtained only qualitative agreement between their calculations and the experimental results.

A reliable way to address the relationship among size, shape and ordering temperature is an ab initio + DMFT approach. However, such calculations are extremely time consuming for nanostructures with more than a hundred atoms.

In this study we focus on finding how the effective nearest neighbors number (z_{eff}) of a nanostructure and its ordering temperature (T_c) reach the bulk limit for different sample geometries, i.e. we explore the boundary between the nanoscopic and the microscopic behavior. For this purpose we go beyond the Ising Model and develop a quantum Heisenberg-Variational approach combining a free energy variational method, based on the Bogoliubov inequality, with a three dimensional (3D) Heisenberg model involving quantum spin pair correlations (Orstein-Zernike correlations). The former, as energy minimization tool, has already been successfully employed for describing the properties of magnetic systems where theoretical phase diagrams are in good agreement with experimental ones [24–26]. Besides this method is simple and fast, it reveals the essential contributions of size and shape to the ordering temperature in nanostructures.

Hereafter we present the theoretical basis and the numerical framework of the method, present and discuss the relevant results and contrast them with available experimental and analytical reports to test its reliability, and finalize with a summary of the conclusions.

2 Theoretical and numerical approach

In the following we describe the theoretical details of our method that gives place to a relationship between the pseudo-critical temperature; which, hereafter we will refer to as ordering temperature, and the effective coordination number on the nanostructures, and, consequently, with the geometry and the crystalline lattice. The general system we consider consists of magnetic nanoparticles composed of N atoms described by a quantum Heisenberg Hamiltonian $\mathcal{H} = -\sum_{\langle i,j\rangle} J_{ij}\mathbf{S}_i\cdot\mathbf{S}_j$. In this expression the sum runs over nearest neighbor atoms $\langle i,j\rangle$, $\mathbf{S}_i$ represents the spin operator for the ith atom, and J_{ij} denotes the exchange coupling between nearest neighbor spins. In this study, such values are kept fixed in most of the results as $J_{ij} = J = 6.62$ meV and $S = 2$. These values reproduce the bulk $T_c(\infty)$ value for bcc Fe, and have been selected for comparison purposes. However the method is valid for any material represented by particular values of S and J, as can be seen in the final section of this paper, where we present a comparison with experimental results of Ni nanowires and other models.

As it is known, it is possible to obtain approximate thermodynamic properties of statistical systems based on a variational principle for the free energy [21–23].

In the procedure, which involves the choice of a suitable parametrized trial Hamiltonian accounting for some elementary interactions, a cluster-spin approach is used. As a first approximation we consider here the Oguchi cluster method consisting in considering pairs of spins to describe the sample. Then, in this spin pairs approximation the system can be considered as formed by n_1 single spins (S) and n_2 linked pairs (P) of spins with a total number of spins $N = n_1 + 2n_2$. Thus, a trial Hamiltonian can be written as

$$\mathcal{H}_0 = -\gamma_s \sum_{i}^{n_1} S_{iz} - \sum_{j,k\in pairs} J_{jk}\mathbf{S}_j\cdot\mathbf{S}_k - \gamma_p \sum_{j\in pairs} S_{jz}, \quad (1)$$

where γ_s and γ_p are variational parameters that can be interpreted as molecular fields to be determined from energy minimization conditions. Here, the first summation runs over single spins and the second and third ones run over spins belonging to pairs. Both Hamiltonians, the original one used to model our system and the trial Hamiltonian recently described, can be related through a variational approach based on the Bogoliubov inequality

$$F \leq F_0 + \langle \mathcal{H} - \mathcal{H}_0\rangle_0 \equiv \Phi, \quad (2)$$

where F is the Helmholtz Free Energy defined by $\mathcal{H}$, F_0 is the free energy defined by $\mathcal{H}_0$, and $\langle ...\rangle_0$ refers to the thermal average on the ensemble defined by $\mathcal{H}_0$.

Now we need to minimize Φ. Taking into account the mean value for an observable and considering statistical independence of the spins, i.e. $\langle \mathbf{S}_i\cdot\mathbf{S}_j\rangle_0 = \langle \mathbf{S}_i\rangle_0\langle \mathbf{S}_j\rangle_0$, and defining the magnetization as $m = \langle \mathbf{S}_{iz}\rangle$ (since, due to spin precession $\langle \mathbf{S}_{ix}\rangle = \langle \mathbf{S}_{iy}\rangle = 0$), we get

$$\langle \mathcal{H} - \mathcal{H}_0\rangle_0 = -Jn'm^2 + (N - 2n_2)m\gamma_s + n_2Jm^2 + 2n_2m\gamma_p, \quad (3)$$

where n' is the number of nearest neighbors. According to the way the system has been figured out we have $F_0 = -k_B T \ln(Z_S Z_P)$, where

$$Z_S = \sum_{\{S\}} e^{-\beta\left(-\gamma_s \sum_i S_{iz}\right)},$$

$$Z_P = \sum_{\{P\}} e^{-\beta\left(-J\sum_{jk} \mathbf{S}_j \cdot \mathbf{S}_k - \gamma_p \sum_j S_{jz}\right)}$$

are the trial partition functions for single and paired spins in the system, respectively.

Although the Oguchi cluster method [27] does not account for long-range fluctuations, here we go a step forward looking for accuracy and consider Ornstein-Zernike correlations [28–30], i.e. correlations between spin pairs. Superior order calculations could go beyond the spin pairs approximation and consider sets of 3, 4, 6 or more spins correlated, which will imply bigger analytical efforts. Results and comparisons discussed below, however, show that spin pair correlation is a good enough approximation keeping calculation requirements under reasonable limits. Since $\mathbf{S}_j$ and $\mathbf{S}_k$ represent spin quantum operators, the eigenvalues of the Hamiltonian have to be computed in the vector space of the two spins. Therefore, computation of partition functions requires vector space analysis in order to obtain the eigenvalues for each Hamiltonian accordingly to the spin values involved. Following this procedure, the calculation of F_0 and $\langle \mathcal{H} - \mathcal{H}_0 \rangle_0$ leads to the minimization of the energy (i.e. $\partial \Phi / \partial m = 0$), giving

$$-2n'Jm + (N - 2n_2)\gamma_s + 2n_2 Jm + 2n_2 \gamma_p = 0.$$

In this expression n', the number of nearest neighbors, depends on the crystalline structure, on the shape and on the size of the system. Since due to the variational principle Φ diminishes as n_2 increases, we take n_2 as large as physically possible, i.e. $n' = n_2$. Thus, the number of linked pairs is maximized to n'. Hence we obtain the following relationship between the variational parameters or molecular fields γ_s and γ_p,

$$\gamma_s = \frac{(2\gamma_p n'/N)}{(2n'/N) - 1} = \frac{\gamma_p z_{\mathit{eff}}}{z_{\mathit{eff}} - 1}, \tag{4}$$

where $z_{\mathit{eff}} = 2n'/N$ can be interpreted as an effective coordination number, and exhibits a strong dependence on crystallinity, shape and size.

Additionally, the method takes advantage of the fact that the magnetization of the system can, indistinctly, be obtained either from single spins (m_S) or from spins belonging to a pair (m_P), that is

$$m = \frac{1}{\beta}\frac{\partial \ln Z_s}{\partial \gamma_s} = \frac{1}{2\beta}\frac{\partial \ln Z_p}{\partial \gamma_p}. \tag{5}$$

After calculating the derivatives and taking into account the computation of the twenty five eigenvalues resulting from the tensor product $\mathbf{S}_i \otimes \mathbf{S}_j$ between the spins, we obtain the following transcendental equation for the magnetization for the case considered here ($\mathbf{S} = 2$)

$$m = \frac{2\sinh 2\beta\gamma_s + \sinh \beta\gamma_s}{1 + 2\cosh 2\beta\gamma_s + 2\cosh \beta\gamma_s} = \frac{B}{4Z_p}, \tag{6}$$

where

$$\begin{aligned} B = {} & 6\sinh 3\beta\gamma_p + 4\sinh 2\beta\gamma_p + 2\sinh \beta\gamma_p \\ & + 2e^{-5\beta J}\sinh \beta\gamma_p + e^{-3\beta J}\left(4\sinh 2\beta\gamma_p + 2\sinh \beta\gamma_p\right) \\ & + e^{4\beta J}(8\sinh 4\beta\gamma_p + 6\sinh 3\beta\gamma_p \\ & + 4\sinh 2\beta\gamma_p + 2\sinh \beta\gamma_p), \end{aligned}$$

and

$$\begin{aligned} Z_p = {} & 1 + 2\cosh 3\beta\gamma_p + 2\cosh 2\beta\gamma_p + 2\cosh \beta\gamma_p \\ & + 2e^{-5\beta J}\cosh 2\beta\gamma_p + 2e^{-3\beta J}\cosh 2\beta\gamma_p \\ & + 2e^{-3\beta J}\cosh \beta\gamma_p + 2e^{4\beta J}\cosh 2\beta\gamma_p \\ & + 2e^{4\beta J}\cosh 4\beta\gamma_p + 2e^{4\beta J}\cosh 3\beta\gamma_p \\ & + 2e^{4\beta J}\cosh \beta\gamma_p + e^{-6\beta J} + e^{-5\beta J} + e^{-3\beta J} + e^{4\beta J}. \end{aligned}$$

Here, $\beta = (k_B T)^{-1}$. From equations (4) and (6) we can obtain numerically the magnetization as a function of the temperature for different system sizes, and then obtain the size dependence of the ordering temperature T_c when we impose $m = 0$.

It is also possible to derive an analytical expression for the ordering temperature (T_c) from equation (6), by taking the limits $\gamma_p \to 0$ and $\gamma_s \to 0$. This yields the following expression

$$\frac{z_{\mathit{eff}}}{z_{\mathit{eff}} - 1} = \frac{14 + e^{-5\beta_C J} + 5e^{-3\beta_C J} + 30e^{4\beta_C J}}{14 + 6e^{-5\beta_C J} + 10e^{-3\beta_C J} + 18e^{4\beta_C J} + 2e^{-6\beta_C J}}, \tag{7}$$

where $\beta_C = (k_B T_c)^{-1}$. By defining $z' = (z_{\mathit{eff}} - 1)/z_{\mathit{eff}}$ and $X = e^{J\beta_C}$, equation (7) transforms into

$$6(5z' - 3)X^{10} + 14(z' - 1)X^6 + 5(z' - 2)X^3 + (z' - 6)X - 2 = 0, \tag{8}$$

whose positive real solution we will denote by Φ_0. This expression connects the ordering temperature with the effective coordination number (z_{eff}) and leads us to compute T_c for different geometries as function of size. With this in mind we obtain an expression for the implicit dependence of T_c on z_{eff},

$$T_c = 11.6279 J/(\ln \Phi_0). \tag{9}$$

It is worthwhile noting that Φ_0 depends on the effective coordination and, consequently, on the geometry and the crystalline lattice of the sample under study.

Finally, it is worth mentioning that low-temperature quantum fluctuations have non-negligible effects in low-dimensional systems e.g. they can avoid or destroy magnetic order in one-dimensional systems. However, once the dimensionality of the system increases their effects are offset by the exchange couplings and bigger coordination, and order can be obtained (as in 2-D and 3-D samples at low-temperature regime). Here we consider nanometric systems and study the size, crystalline structure and shape effects through the use of an effective coordination number z_{eff}, for which the spin-spin correlations are computed in a short-range (pair) approximation. From a phase diagram

in terms of z_{eff} (not shown), magnetic transition are observed just above the value z_{eff} =2.5. This result indicates that, at very small sizes (corresponding in fact to low-dimensionality) no magnetic order is observed. However, for bigger values of the effective coordination number magnetic order is obtained, and the model can be employed.

3 Results and discussion

We focus our analysis on the size dependence of the ordering temperature and the effective coordination number. As a first step we consider spherical particles crystallizing in simple cubic (sc), body centered cubic (bcc) and face centered cubic (fcc) lattices. We start our calculations obtaining the values for z_{eff} as a function of the diameter Da of the sphere for each crystalline lattice, where a is the lattice parameter and D is a dimensionless quantity. Since, due to the discrete character of the sample, the number of atoms inside a sphere (and therefore the number of bonds among those atoms) is not given by an exact equation, we made numerical calculations for spheres of several sizes and adjust them to simple expressions that can be easily calculated. The resultant functional forms are similar to the one obtained when the analytical calculation is implemented for cubes; for spheres this leads to

$$z_{eff} = \frac{8\left(6+\frac{3}{D-0.7}\right)}{\left(1+\frac{1.08}{D-0.7}\right)^3+3+\frac{3}{D-0.7}} \quad \text{fcc}, \tag{10}$$

$$z_{eff} = \frac{16}{\left(1+\frac{0.87}{D}\right)^3+1} \quad \text{bcc}, \tag{11}$$

$$z_{eff} = \frac{6}{\left(1+\frac{1.5}{D-1.36}\right)} \quad \text{sc}. \tag{12}$$

These expressions, with $D \to \infty$, tend to the bulk behavior. In this case and using J = 6.62 meV, the ordering temperatures for bulk, $T_c(\infty)$ become 1665.04 K for fcc, 1043.03 K for bcc and 728.20 K for sc structures. For comparison purposes we normalize T_c by the corresponding $T_c(\infty)$.

By using the expressions for z_{eff} as functions on the dimensions for the different lattice types, we can obtain the size dependence of z_{eff} and T_c. Such dependences for fcc, bcc and sc spheres are shown in Figure 1. As observed, a similar behavior is obtained in all the particles that reach the bulk limit for D close to 10^3.

Despite this, the differences among the three lattices in T_c and z_{eff} are small at smaller sizes, and increase continuously until the particles reach the bulk limit. Differences among the three lattices are notable, being larger the one obtained between the fcc and bcc structures; these differences reveal that the tendency of the different lattices toward the bulk behavior takes place at different rates.

Comparing both quantities, z_{eff} and T_c, two different effects have to be highlighted; (i) the faster tendency of the z_{eff} toward the bulk behavior as the size increases in comparison with the behavior of $T_c(D)$; and (ii) the major separation among the $T_c(D)$ curves as compared with those for $z_{eff}(D)$. This effect is the result of the logarithmic relationship between T_c and z_{eff} evidenced in equation (9). These features indicate the clear effect of the crystalline lattice on the magnetic behavior of systems at these nanometric scales whenever they approximate the bulk condition.

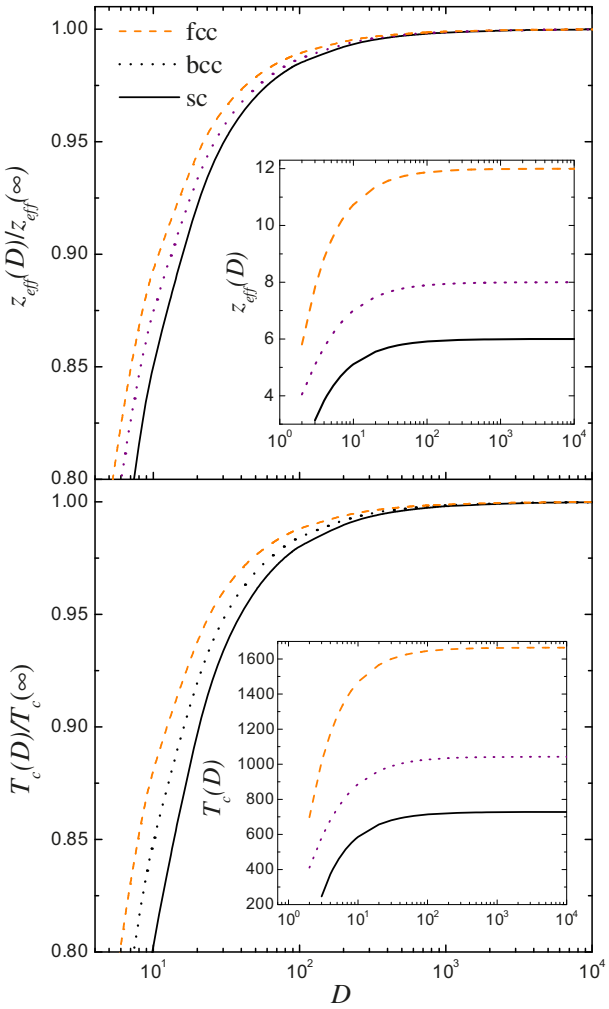

Fig. 1. Size dependence of the reduced coordination number (top) and the reduced ordering temperatures (bottom) as a function of the diameter D for fcc, bcc and sc spheres. Insets show the corresponding not normalized $z_{eff}(D)$ and $T_c(D)$ curves to illustrate the different behavior for the different crystalline lattices.

Since the behavior of z_{eff} and T_c are very similar, and considering that T_c is the measurable quantity, in what follows we will show results only for this last magnitude.

Once clarified the role of the lattice and the coordination number, for simplicity we continue our calculations considering only bcc structures and focusing on the effect of the geometry on the ordering temperature. We consider now cylinders of heigh La and diameter Da (i.e. L and D are given in lattice constants), and as in the previous case of spheres, we fit the numerical calculations for z_{eff}

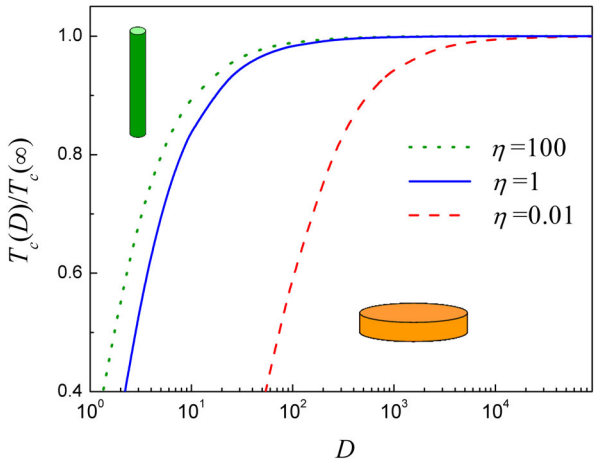

Fig. 2. Size dependence of T_c for bcc cylinders of different selected values of the aspect ratio η. η >1 corresponds to nanowire-like structures while $\eta < 1$ represents dots.

for several sizes to a simple expression similar to the one obtained when the analytical calculation is implemented for parallelepipeds. For bcc cylinders, this leads to

$$z_{eff} = \frac{16}{\left(1+\frac{0.92}{D}\right)^2\left(1+\frac{0.98}{L}\right)+1}. \quad (13)$$

Figure 2 illustrates our results for cylinders of different aspect ratio $\eta = L/D$. Here $\eta < 1$ represents dots and $\eta > 1$ denotes wire-like structures. In spite for dots the effect of the geometry is evident, as can be seen by looking at the separation between the curves for $\eta = 0.01$ and $\eta = 1$, the effect is less important when considering wires. Results for larger values of η (η >100) almost coincide with the curve for η = 100. For dots the size effects just appear until reaching $D \approx 10^4$, while for large aspect ratios the size effects appear until reaching $D \approx 10^2$.

More information about the behavior of cylindrical particles can be obtained from Figure 3, that represents a three dimensional graph for T_c as a function of both D and L simultaneously. This figure reveals the existence of critical diameters and lengths at which the system does not reach the T_c bulk, regardless the size of the other dimension. This means that, if one dimension is small enough, it determines the behavior of the system.

To understand this behavior we study the thermal dependence of the correlation length of the system, given by [31]:

$$\xi = \frac{a'}{\sqrt{z_{eff}}}\left(1-\frac{T}{T_{c\_M=0}}\right)^{\nu} \quad (14)$$

where $a' = 2.47$ for Fe bcc, z_{eff} responds for the effective coordination of the nanoparticles of different size, $T_{c\_M=0}$ is the corresponding ordering temperature, and $\nu = 0.71$ is the critical exponent for a three dimensional Heisenberg spin model [31]. In Figure 4 we present graphically the behavior of the correlation length as a function of temperature for spherical nanoparticles of selected sizes. As observed, the correlation length reveals a monotonous increasing behavior, diverging asymptotically for the value

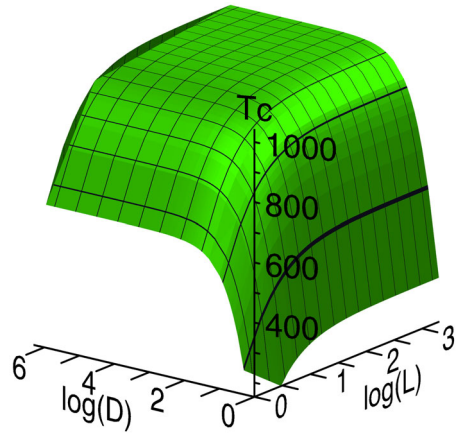

Fig. 3. Size dependence of T_c for bcc cylinders as a function of both the diameter D and length L. The figure illustrates the different behaviors for diameter and length, and the expected plateau in T_c for big values of the dimensions. Lateral hillsides indicate that whenever one of the dimensions of the nanostructure is small, independently of how big the other dimensions become, temperature saturates at smaller values than the one corresponding to the observed plateau i.e. the system does not exhibit bulk-like behavior.

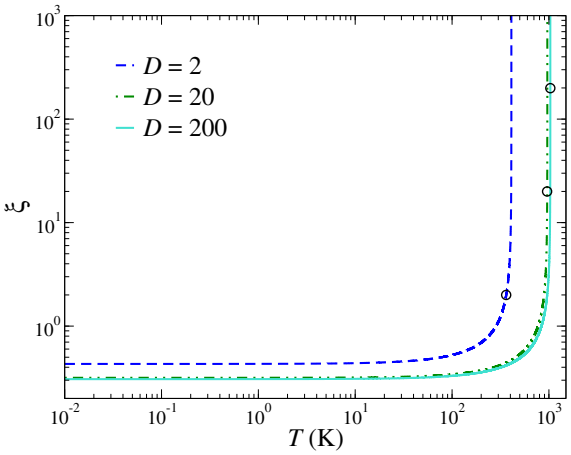

Fig. 4. Thermal dependence of the correlation length (in nm) for spherical nanoparticles of different selected sizes (D in unit cells). Black open circles indicate the ordering temperatures computed from the correlation length criterion (see text) which are slightly different to those indicated by the divergence of correlation length ($T_{c\_\xi\to\infty}$).

of the ordering temperature $T_{c\_M=0}$. As it is well know, whenever a bulk system is reaching its critical temperature, correlation length diverges ($\xi \to \infty$), and magnetic order disappears.

Therefore, two different definitions could be considered for the ordering temperature in the thermodynamic limit. (i) From a M vs. T graph: ordering temperature is that temperature for which the first zero is obtained in magnetization M while increasing temperature in the graph M vs. T. (ii) From the correlation length T_{c_ξ}: ordering temperature is that temperature for which the value of

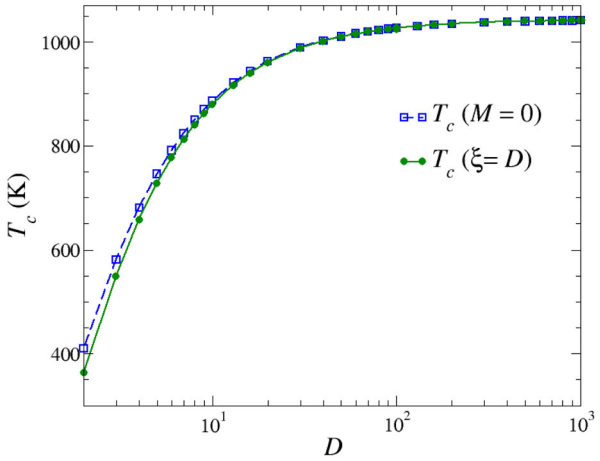

Fig. 5. Ordering temperature as a function of size computed from the two definitions (see text) coming from $M = 0$ (squares) and from the correlation length criterion $\xi = D$ (circles).

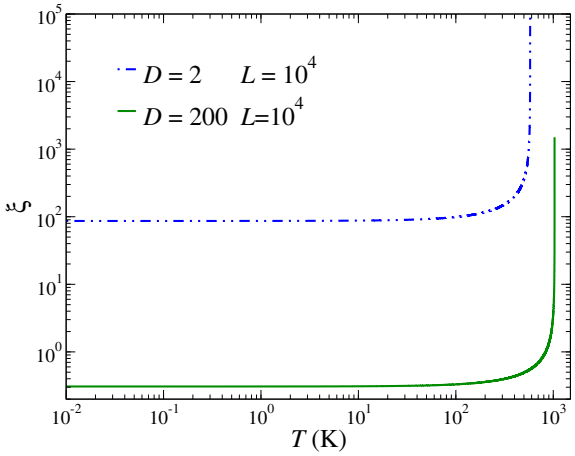

Fig. 6. Thermal dependence of ξ for cylinders of two different aspect ratios (D and L in unit cells). As observed, $\xi \sim 100$ for the cylinder with diameter $D = 2a$ (discontinuous line), indicating that a portion of the spins of the system are correlated, and no order is obtained in the sample.

the correlation length diverges. Both of these definitions lead to the same value for the ordering temperature in the bulk case ($T_{c\_bulk} = T_{c\_M=0} = T_{c\_\xi\to\infty}$).

On the other hand, for confined systems, if correlation length reaches values equal or greater than the size of the sample, the spins are correlated at all, which is equivalent to the bulk case ($\xi = \infty$). Then, from case (ii) of the last paragraph applied to a nanostructure, ordering temperature will take place whenever correlation length equates the size of the nanostructure ($\xi = D$). In other words, since the system size is finite, whenever the correlation length gets bigger values than its size, the whole system will be governed by fluctuations, i.e. this finite value for ξ, in a practical way, will not be different from $\xi \to \infty$ for the element. This gives place to different values for the ordering temperature of the nano-system as defined in (i) and (ii); as indicated by open black circles in Figure 4.

The differences between the ordering temperatures computing from the two definitions are evident for very small sizes and progressively decrease as the system size increases. Figure 5 shows the comparison between the two definitions of the ordering temperature as function of the size for nanospheres.

This can lead to think in a non-abrupt magnetic phase transition occurring in a certain region defined as ($T_{c\_M=0} - T_{c\_\xi=D}$). Moreover, taking advantage of these differences between the ordering temperature definitions, an adequate definition for the nanoscopic-macroscopic boundary as size is increasing could be that size for which both ordering temperatures coincide (i.e. $T_{c\_M=0} = T_{c\_\xi=D}$) within the experimental uncertainty ∼1 K.

Now, from this analysis it is possible to understand the result reported in Figure 7 for cylinders with a fix dimension. Lateral hillsides observed in that figure indicate that whenever one of the dimensions of the nanostructure is small, independently of how big the other dimensions become, temperature saturates at smaller values than the one corresponding to the observed plateau i.e. the system

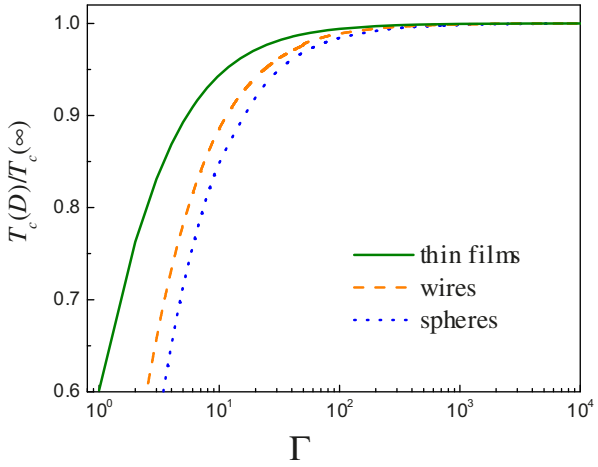

Fig. 7. Size dependence of T_c for thin films (quasi-2D), wires (quasi-1D) and dots (quasi-0D) in the bcc lattice.

does not exhibit bulk-like behavior. As observed in Figure 6, for a system with a very small fix diameter (let us say $D = 2a$) the correlation length at any temperature gets a value greater than the diameter ($D \sim 100$ in this case). The spins in the systems, at least in a certain region, are correlated and, consequently, the system will not be completely ordered at any temperature.

Furthermore, it can be seen the asymmetry in the rate of approaching the bulk behavior. As the diameter is varied at a fix length, the tendency towards the bulk is slower than when varying the length at a fix diameter. This behavior is due to the relation between z_{eff} and D and L, expressed in equation (13).

Now we explore the effect of dimensionality by comparing the behavior of (i) cylinders with a length going to infinity and varying the base diameter (pseudo-one dimensional particles); and (ii) thin films with a circular base of diameter going to infinity (pseudo-two dimensional

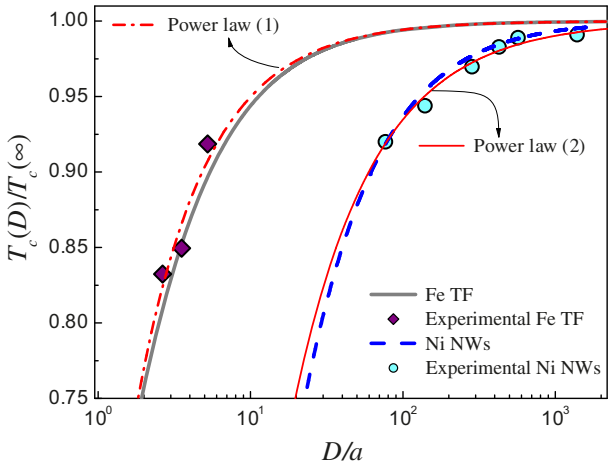

Fig. 8. Comparison among experimental data and results of our model for the size dependence of T_c for Fe thin films (brown line) and Ni nanowires (blue dashed line). Remarkable agreement is obtained with experimental results available for Fe thin films (violet diamonds) of reference [32] and Ni nanowires (cyan dots) of reference [14]. This figure also shows the corresponding fit functions to the experimental data by using a power law function resembling a Finite Size Scaling behavior. Power law (1) corresponds to the function used to fit Fe thin film data (purple diamonds), and the values for the best fitting parameters are $\nu = 1.06 \pm 0.42$ and $d_0 = 0.42 \pm 0.34$. Power law (2) corresponds to the best fit to Ni nanowires (cyan circles) with values given by $\nu = 1.21 \pm 0.11$ and $d_0 = 3.7 \pm 1.1$.

particles) varying its thickness. We also include spheres, that can be considered as pseudo-zero dimensional structures. The finite dimensions will be denoted by Γ. Our results are depicted in Figure 7 showing that, in spite of having one or two dimensions of infinite size, the effect of the other finite dimensions is evident as mentioned previously. To illustrate the differences between the three behaviors we calculate the values of Γ that are needed to have $T_c = 0.9T_c(\infty)$ and found $\Gamma = 5.5$ for the thin films, $\Gamma = 11.5$ for the cylinders and $\Gamma = 16$ for the spheres. Such differences in Γ account for the distinct geometries. The existence of two dimensions going to infinity is responsible of a faster increase of T_c as compared with the cylinder case.

In order to validate our model we compare our results for Fe films and Ni nanoparticles with experimental results from Qiu et al. [32] and Sun et al. [14], respectively. For the latter case we consider the corresponding data for Ni, i.e. $J_{i,j} = J = 22.067$ meV, $T_c(\infty) = 631$ K, $S = 1/2$ and a fcc lattice with parameter $a = 0.352$ nm. In this case, the functional $T_c(z_{eff})$ relationship reads as [21]

$$T_c = Jk_B^{-1}\left(\ln\frac{z_{eff}}{z_{eff}-4}\right)^{-1}. \quad (15)$$

Very good agreement with experimental results is observed (see Fig. 8). This indicates that our model, that has no adjustable parameters, describes adequately these nanostructures.

Finally, as a second way of validation, we have taken into account other models describing the size dependence of the ordering temperature in nanostructures from an analytical perspective [33,34]. First, in 2003, Nikolaev and Shipilin considered the ordering temperature as proportional to the mean number of exchange bonds per unit volume and proposed a one-parameter model for the size dependence of T_c [33]

$$T_c(D)/T_c(\infty) = 1 - (3\Delta t_s)/(2D), \quad (16)$$

where Δt_s is the thickness of the surface layer, which contains the dangling bonds, and characterizes the effect of the presence of surface on the ordering temperature of the system. Later, in 2006, Lang et al. added a new parameter and presented a model to describe the mechanisms lying on the effect of the breaking of exchange bonds upon the $T_c(D)$ function for nanostructures [34]. Such two-parameter model gives the following expression,

$$T_c(D)/T_c(\infty) = \exp\left[-(\alpha-1)/(D/D_0-1)\right], \quad (17)$$

where α is a measure of the root-mean-square thermal average amplitude of the surface atom vibration relative to the core and D_0 denotes a critical size at which all atoms of the nanostructure are located on its surface. As reported in that reference, whenever nanoparticles and wires are considered, the mentioned models adopted the following parameters values. Nicolaev's model uses $\Delta t_s = 0.6078$ and $\Delta t_s = 0.4052$ for spheres and wires, respectively. While the Lang's model uses $\alpha = 1.612$ and $D_0 = 1.4898$ for spherical nanostructures, and $\alpha = 1.612$ and $D_0 = 0.9932$ for the wire-like case [33,34].

Moreover, since it is often to find comparisons among these size dependent behaviors and functions inspired in Finite Size Scaling Theory, we have performed a simple analysis. To do this we considered the following expression resembling a finite size behavior [35,36]:

$$T_c(D)/T_c(\infty) = 1 - (D/d_0)^{-1/\nu}; \quad (18)$$

where d_0 and ν are the fitting parameters (ν resembling a critical exponent). With this in mind, the resultant values for the best fit to the experimental data are: $d_0 = 0.42 \pm 0.34$ and $\nu = 1.1 \pm 0.4$ for the Fe thin films; and $d_0 = 3.7 \pm 1.1$ and $\nu = 1.2 \pm 0.2$ for the Ni nanowires. As expected, the values for ν are in accordance with a Heisenberg-like model.

The comparison among our model for spherical nanoparticles and nanowires and the mentioned analytical models is presented in Figure 9. As observed, the three models discussed exhibit a very good qualitative agreement. Differently to the two mentioned models, ours gives smaller values for the T_c in the range studied, and presents a slower tendency to the bulk conditions as the size increases. Furthermore, as observed in Figure 8, our approach results in an excellent description of the experimental results.

The good agreement obtained among our results and those reported in literature both experimental and analytically [14,32–34] indicates that the Heisenberg-Variational

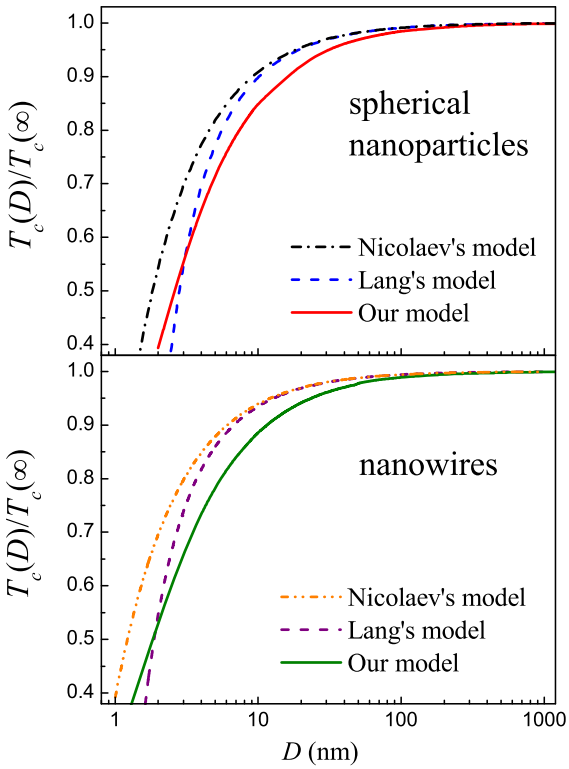

Fig. 9. Comparison with theoretical models presented in references [33,34] for spherical and wire-like nanostructures. Nicolaev's model (dashed lines) uses $\Delta t_s = 0.6078$ and $\Delta t_s = 0.4052$ for spheres and wires, respectively. While the Lang's model uses $\alpha = 1.612$ and $D_0 = 1.4898$ for spherical nanostructures (dot-dashed lines), and $\alpha = 1.612$ and $D_0 = 0.9932$ for the wire-like case (dot-dot-dashed lines) [33,34]. Solid lines represent results of our model.

Energy approach proposed here can be considered as a reliable and useful scheme for obtaining magnetic properties of systems at the nanometric range of sizes.

4 Conclusions

The last years have brought a great interest in the ordering temperature of nanostructures, offering the possibility of exploring them from different perspectives. A general methodology that can be applied to study materials with different spin values, and the size and shape dependences of the ordering temperatures for nanostructures has been presented in this study. Despite its simplicity, from the comparison with experimental results, we can be confident that it reveals the essential contributions of size and shape to the ordering temperature. To sum up, we have proposed a quantum Heisenberg-Variational Energy scheme to investigate the behavior of nanoparticles with different geometries and crystalline lattices as a function of their size. According to our results, the particles reach the bulk limit at different sizes depending on their geometry. These results also suggest that the nano-bulk limit is located at about 10^2a–10^3a, in most of the cases. The confidence of our model has been tested by comparisons with other experimental [14,32] and analytical [33,34] reports. Finally, it is worthwhile mentioning that results presented here might bring the attention of experimental researchers interested in issues related to the size, shape and crystalline lattice dependence of the ordering temperature in nanometric systems.

This work was supported in Colombia by the IN10221CE and IN10197CE SUI projects of the GICM and GES Groups at Universidad de Antioquia (UdeA). In Chile we received support through FONDECYT Grants 1130672 and 1120356; the Millennium Science Nucleus "Basic and Applied Magnetism" P010-061F, "Financiamiento Basal para Centros Científicos y Tecnológicos de Excelencia" Grant FB0807 and AFOSR Grant FA9550-11-1-0347. J.M.-Z. thanks UdeA for a "Dedicación Exclusiva 2013-2014" program. We are deeply indebted with Prof. D. Givord for a critical reading of the manuscript followed of very interesting discussions. We are also grateful with Dr. L.F. Duque and the two anonymous reviewers for their helpful comments and suggestions.

References

1. C.V. Salata, J. Nanobiotechnology **2**, 3 (2004)
2. Q.H. Wang, K. Kalantar-Zadeh, A. Kis, J.N. Coleman, M.S. Strano, Nature Nanotechnology **7**, 699 (2012)
3. M. Imran, A.M. Revol-Junelles, A. Martyn, E.A. Tehrany, M. Jacquot, M. Linder, S. Desobry, Critical Reviews Food Science Nutrition **50**, 799 (2010)
4. F. Sun, K.A. Osseo-Asare, Y. Chen, B.A. Dempsey, J. Hazardous Mater. **196**, 311 (2011)
5. R. Skomski, J. Phys.: Condens. Matter **15**, R841 (2003)
6. E.L. Lee, P.E. Bolduc, C.E. Violet, Phys. Rev. Lett. **13**, 800 (1964)
7. F. Huang, G.J. Mankey, M.T. Kief, R.F. Willis, J. Appl. Phys. **73**, 6760 (1993)
8. T. Ambrose, C.L. Chien, Phys. Rev. Lett. **76**, 1743 (1996)
9. Y.T. Chen, S.M. Xie, J. Nanomaterials **2012**, 486284 (2012)
10. D. Tobia, E. Winkler, R.D. Zysler, M. Granada, H.E. Troiani, Phys. Rev. B **78**, 104412 (2008)
11. E.G. Moshopoulou, O. Isnard, M. Milanovic, V.V. Srdic, Probing the Transition from Nano-to Bulk-Like Behaviour in $ZnFe_2O_4$ Nanoparticles, in *Materials Science Forum* (Trans Tech Publ, 2011), Vol. 674, pp. 207–211
12. X. Batlle et al., J. Appl. Phys. **109**, 07B524 (2011)
13. D.H. Han, J.P. Wang, H.L. Luo, J. Magn. Magn. Mater. **136**, 176 (1994)
14. L. Sun, P.C. Searson, C.L. Chien, Phys. Rev. B **61**, R6463 (2000)
15. L. Sun, C.L. Chien, P.C. Searson, J. Mater. Sci. **35**, 1097 (2000)
16. J. Meier, B. Doudin, J.P. Ansermet, J. Appl. Phys. **79**, 6010 (1996)
17. M.G. Krishna, A.K. Kapoor, M.D. Prasad, V. Srinivasan, Physica E **33**, 359 (2006)
18. M.G. Krishna, A.K. Kapoor, M.D. Prasad, V. Srinivasan, Physica E **42**, 1920 (2010)

19. D.S. Bertoldi, E.M. Bringa, E.N. Miranda, J. Phys.: Condens. Matter **24**, 226004 (2012)
20. E.A. Velásquez, J. Mazo-Zuluaga, J. Restrepo, Ò. Iglesias, Phys. Rev. B **83**, 184432 (2011)
21. L.G. Ferreira, S.R. Salinas, M.J. Oliveira, Phys. Stat. Sol. B **83**, 229 (1977)
22. J.R. Faleiro Ferreira, N.P. Silva, J. Phys. A **20**, 6429 (1987)
23. J.R. Faleiro Ferreira, Phys. Stat. Sol. B **148**, 709 (1988)
24. D. Peña Lara, G.A. Pérez Alcázar, L.E. Zamora, J.A. Plascak, Phys. Rev. B **80**, 014427 (2009)
25. J. Restrepo, G.A. Pérez Alcázar, Phys. Rev. B **61**, 5880 (2000)
26. A. Osorio, W.R. Aguirre Contreras, L.E. Zamora, G.A. Pérez Alcazar, J.A. Plascak, Phys. Rev. B **68**, 024420 (2003)
27. S. Smart, *Effective field theories of magnetism*, 1st edn. (Saunders Co., Philadelphia, 1966)
28. J.M. Yeomans, *Statistical mechanics of phase transitions*, 1st edn. (Oxford Science Publications, New York, 1992)
29. R. Skomski, *Simple models of magnetism*, 1st edn. (Oxford Graduate Texts, New York, 2008)
30. H.E. Stanley, *Introduction to phase transitions and critical phenomena*, 1st edn. (Oxford University press, New York, 1971)
31. R. Skomski, D.J. Sellmyer, J. Appl. Phys. **87**, 4756 (2000)
32. Z.Q. Qiu, J. Pearson, S.D. Bader, Phys. Rev. Lett. **70**, 1006 (1993)
33. V. Nikolaev, A. Shipilin, Phys. Solid State **45**, 1079 (2003)
34. X.Y. Lang, W.T. Zheng, Q. Jiang, Phys. Rev. B **73**, 224444 (2006)
35. D.R. Ritchie, M.E. Fisher, Phys. Rev. B **7**, 480 (1973)
36. F. Huang, G.J. Mankey, M.T. Kief, R.F. Willis, J. Appl. Phys. **73**, 6760 (1993)